Acta Cryst E CRYSTALLOGRAPHIC COMMUNICATIONS

ISSN 2056-9890

A redetermination of the structure and Hirshfeld surface analysis of poly[diaquadi-μ-hydroxido-tetrakis(μ-nicotinato *N*-oxide)tricopper(II)]

Masoud Mirzaei,[a]* Maryam Bazargan,[a] Pouria Ebtehaj[a] and Joel T. Mague[b]

[a]Department of Chemistry, Faculty of Science, Ferdowsi University of Mashhad, 9177948974, Mashhad, Iran, and [b]Department of Chemistry, Tulane University, New Orleans, LA 70118, USA. *Correspondence e-mail: mirzaeesh@um.ac.ir

Received 20 January 2021
Accepted 19 February 2021

Edited by V. Jancik, Universidad Nacional Autónoma de México, México

Keywords: crystal structure; nicotinic acid N-oxide; copper; hydrogen bond.

CCDC reference: 2063970

Supporting information: this article has supporting information at journals.iucr.org/e

The product obtained from the reaction of pyridine-2,3-dicarboxylic acid and hydrated copper(II) chloride in hot aqueous NaOH solution was determined by low temperature X-ray diffraction to be $[Cu_3(C_6H_4NO_3)_4(OH)_2(H_2O)_2]_n$ or $[Cu_3(\mu\text{-}OH)_2(\mu\text{-nicNO})_4(H_2O)_2]_n$ (nicNO is pyridine-3-carboxylate *N*-oxide), a structure obtained from room temperature data and reported previously. The present determination is improved in quality and treatment of the H atoms. A Hirshfeld surface analysis of the intermolecular interactions is presented.

1. Chemical context

N-oxidation of the pyridine ring can significantly increase its electron-donating ability because the charge-polarized pyridine-*N*-oxide moiety can donate three pairs of electrons while a neutral nitrogen atom in pyridine only gives one pair of electrons. Therefore, it is expected that *N*-oxidation can increase the coordination capacities and flexibility of the ligand. Metal complexes of pyridine-*N*-oxide ligands have been found to be particularly useful in the selective adsorption and separation of gases (CO_2 over CH_4) and as anti-HIV and luminescent agents (Noro *et al.*, 2015; Xiong *et al.*, 2014; Balzarini *et al.*, 2005; Lis *et al.*, 2002). These features have motivated our interest in the chemistry of carboxylic acid derivatives of pyridine-*N*-oxide for investigating the influence of the *N*-oxide moiety on the coordination mode(s) in the crystal lattice (Mirzaei *et al.*, 2020; Hosseini-Hashemi *et al.*, 2018, 2019; Bazargan *et al.*, 2016, 2020; Mirzaei, Eshtiagh-Hosseini, Bazargan *et al.*, 2015; Shahbazi *et al.*, 2017; Mirzaei, Eshtiagh-Hosseini, & Bazargan, 2015). Here, we report the isolation and X-ray crystal structure of the coordination polymer $[Cu_3(\mu\text{-}OH)_2(H_2O)_2(\mu\text{-nicNO})_4]_n$ (**1**) (nicNO is pyridine-3-carboxylate *N*-oxide) as the unexpected product from the reaction of pyridine-2,3-dicarboxylic acid with hydrated Cu^{II} chloride. It appears that oxidation and decarboxylation of the starting acid occurred during the reaction, as has been seen previously (Hosseini-Hashemi *et al.*, 2018; Mirzaei, Eshtiagh-Hosseini *et al.*, 2015). During the course of this work, we found two prior reports of this structure [NICTCU (Knuutilla, 1981) and NICTCU01 (Kang *et al.*, 2020)], both obtained with room-temperature data. Overall, the present structure is the same as the previous ones, but with some differences in metrical parameters as a result of the lower temperature of the data collection used here, a lower *R* value [0.0250 for all reflections (3592) *vs* 0.0416 for 2525 with *I*

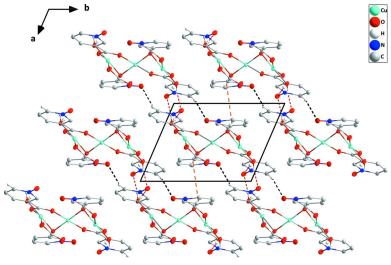

> $3\sigma(I)$ in NICTCU and 0.0538 for 3349 with $I > 2\sigma(I)$ in NICTCU01. The present structure has slightly better s.u.'s on all derived parameters than obtained for NICTCU and significantly better ones than those obtained by Kang *et al.*. One deficiency of the NICTCU structure is the free refinement of hydrogen-atom parameters, a risky procedure with room-temperature data when heavy atoms are present, which led to C—H distances for the aromatic rings varying from 0.97 (2) to 0.84 (3) Å and O—H distances of 0.77 (3) to 0.41 (4) Å, the last three being particularly unrealistic. In addition, there was no absorption correction despite a linear absorption coefficient of 2.422 mm^{-1}. Kang *et al.* performed an absorption correction and treated hydrogen atoms appropriately, but with an R_{int} of 0.0780 their data are clearly of poorer quality than in the present case (R_{int} = 0.0208).

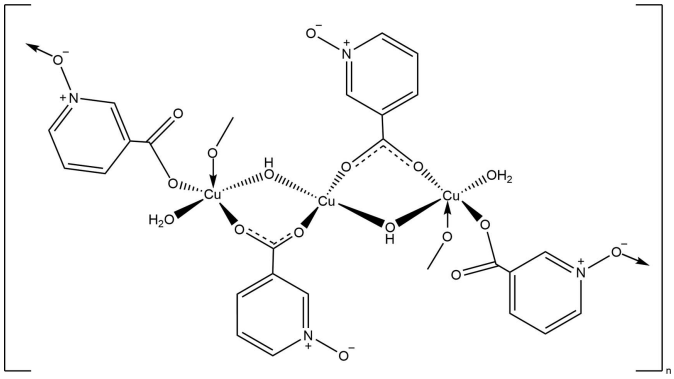

2. Structural commentary

The monomer unit plus one *N*-oxide atom from the bridging nicotinato-*N*-oxido ligand on each end copper atom (O3^{ii} and O3^{iii}) is shown in Fig. 1. This moiety is centrosymmetric with Cu2 lying on the crystallographic center of symmetry. The coordination about Cu1 is square pyramidal with the *N*-oxide atom from the bridging nicotinato-*N*-oxido ligand (O3^{ii}) in the apical site and the basal sites occupied by the bridging hydroxide (O7—H7) and the water molecule (O8) in *trans* positions, and a carboxylate oxygen atom from the bridging nicotinato-*N*-oxido ligand (O1) and the bridging nicotinato-*N*-oxide ligand (O5^{i}). The Cu1—O distances and bond angles are in line with those typically seen for tetragonally elongated, square-pyramidal Cu^{II}. Cu2 is coordinated by the bridging hydroxide (O7—H7) and a carboxylate oxygen of the nicotinato-*N*-oxide ligand (O4) and their symmetry-related counterparts. Although rigorously planar, the coordination about Cu2 shows a rhombic distortion from square geometry due to the difference in the Cu2—O4 [1.9687 (11) Å] and Cu2—O7 [1.9240 (11) Å] bond lengths and the O4—Cu2—O7 angle of 87.69 (5)°. This geometry is quite comparable to those in the previously reported structures (Table 1). One feature noted by Kang *et al.* (2020) but not by Knuutilla (1981) is a weak contact by the *N*-oxide oxygen atoms coordinated to Cu1 (O3^{ii} and O3^{iii}) to Cu2 with the Cu2—O3^{ii} distance of 2.6828 (15) Å being considerably longer than the Cu1—O3^{ii} distance [2.4208 (13) Å] but definitely shorter than the sum of the van der Waals radii (2.92 Å), indicating a short contact. The O7—Cu2—O3^{ii} and O7^{i}—Cu2—O3^{ii} angles of 81.66 (5) and 98.34 (5)°, which differ greatly from 90°, suggest the coordination of Cu2 should not be described as an elongated octahedron. There are close to 100 structures listed in the CSD (Groom *et al.*, 2016) with Cu—O distances of 2.69 Å or greater and we cite three examples close to those observed here: 2.693 (4) Å (Laborda *et al.*, 2004), 2.757 (5) Å (Lazarou *et al.*, 2018) and 2.696 (3) Å (Procházková *et al.*, 2017). In these, the first involves a coordinated water molecule while in the latter

Table 1
Comparison of structures (Å,°).

Metric	This work	NICTCU	NICTCU01
Cu1—O1	1.9542 (12)	1.943 (2)	1.953 (3)
Cu1—O7	1.9003 (12)	1.925 (1)	1.893 (4)
Cu1—O8	1.9539 (12)	1.876 (1)	1.947 (4)
Cu1—O5^{i}	1.9911 (12)	1.979 (2)	1.987 (3)
Cu1—O3^{ii}	2.4208 (13)	2.426 (2)	2.434 (4)
Cu2—O4	1.9687 (11)	1.954 (1)	1.981 (3)
Cu2—O7	1.9240 (11)	1.912 (2)	1.922 (4)
Cu2—O3^{ii}	2.6828 (15)		2.699 (3)
O1—Cu1—O5^{i}	158.98 (5)	158.73 (7)	158.83 (16)
O1—Cu1—O7	97.79 (5)	97.55 (6)	97.87 (14)
O1—Cu1—O8	84.60 (5)	84.84 (6)	84.72 (15)
O7—Cu1—O8	176.16 (5)	176.28 (6)	176.18 (14)
O7—Cu1—O5^{i}	92.38 (5)	92.27 (5)	92.13 (14)
O1—Cu1–O3^{ii}	103.19 (5)	103.56 (7)	103.40 (15)
O7—Cu1—O3^{ii}	89.57 (5)	89.84 (6)	89.24 (15)
O8—Cu1–O3^{ii}	92.82 (5)	92.37 (6)	92.89 (15)
O5^{i}—Cu1—O3^{ii}	95.20 (5)	92.56 (7)	95.31 (14)
O4—Cu2—O4^{i}	180.00 (8)		
O7—Cu2—O4^{i}	87.69 (5)	87.28 (7)	87.79 (15)
O4—Cu2—O7^{i}	92.31 (5)	92.72 (7)	92.21 (15)

Symmetry codes: (i) $-x+1, -y+1, -z+1$; (ii) $x+1, y+1, z$.

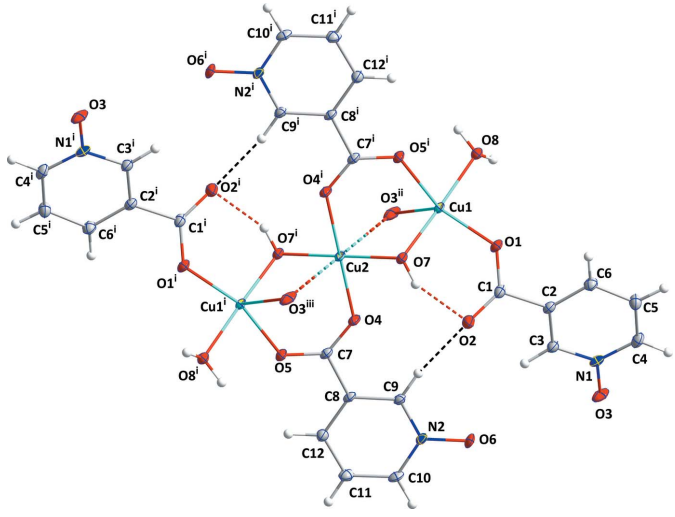

Figure 1
A portion of the title molecule showing the coordination spheres of the independent copper ions with labeling scheme and 50% probability ellipsoids [symmetry codes: (i) $-x+1, -y+1, -z+1$; (ii) $x+1, y+1, z$; (iii) $-x, -y, -z+1$]. O—H···O and C—H···O hydrogen bonds are depicted, respectively, by red and black dashed lines while the weak Cu2···O3^{ii} and Cu2···O3^{iii} interactions are depicted by aqua/red dashed lines.

Table 2
Hydrogen-bond geometry (Å, °).

D—H···A	D—H	H···A	D···A	D—H···A
O7—H7A···O2	0.82 (1)	2.04 (1)	2.8057 (17)	156 (2)
O8—H8A···O6^{i}	0.83 (1)	1.84 (1)	2.6684 (17)	173 (3)
O8—H8B···O6^{ii}	0.84 (1)	1.88 (1)	2.6976 (18)	168 (3)
C9—H9···O2	0.95	2.28	3.216 (2)	168
C10—H10···O3^{iii}	0.95	2.23	3.079 (2)	148

Symmetry codes: (i) $-x+1, -y+1, -z+1$; (ii) $x+1, y+1, z$; (iii) $-x, -y, -z+1$.

two, the distance is to a ligand oxygen atom bridging copper centers and so more comparable to the present work. Where commented on, the long distance is attributed to a Jahn–Teller distortion, but in our case the Cu2—O3^{ii} distance not only is long, but also its direction is tilted away from the Cu2 coordination plane normal by ∼8°. This suggests that O3^{ii} is close to Cu2 for sterical convenience, not due to the formation of a Cu2—O3^{ii} bond. The intramolecular O7—H7A···O2 hydrogen bond (Table 2) belongs to a $S_1^1(6)$ graph set (Bernstein *et al.*, 1995).

3. Supramolecular features

The monomer units, $[Cu_3(\mu\text{-}OH)_2(H_2O)_2(\mu\text{-nicNO})_4]$, are connected into chains extending along the *c*-axis direction by coordination of *N*-oxide oxygen atom O3 to atom Cu1^{i} of the next unit (Fig. 1). The chains are linked into layers parallel to $(1\bar{1}0)$ by pairwise O8—H8A···O6^{i} hydrogen bonds [Table 2 and Fig. 2; graph-set $R_2^2(9)$] together with offset π-stacking between inversion-related C2/C3/N1/C4/C5/C6 rings [centroid–centroid = 3.4753 (13) Å, slippage = 0.53 Å] and inversion-related N2/C9/C8/C12/C11/C10 rings [centroid–centroid = 3.6432 (12) Å, slippage = 1.5 Å] (Fig. 3). The O8—H8B···O6^{ii} hydrogen bond (Table 2) is part of a $C_1^1(11)$ graph set through O4^{ii}, Cu2^{ii}, Cu1^{ii} and O8^{ii} [symmetry code: (ii) $x+1, y+1, z$] as well as a $R_2^2(18)$ graph set through O5^{ii}, Cu2^{ii}, Cu1^{iv}, O8^{iv} and O6^{i} [symmetry codes: (i) $-x+1, -y+1, -z+1$; (iv) $-x+2, -y+2, -z$] and a $C_2^2(22)$ graph set through O4^{ii}, Cu2^{ii}, O4^{v}, O6^{v}, O8^{vi}, Cu1^{vi}, Cu2^{vi}, Cu1^{vii} and O8^{vii} [symmetry codes: (v) $2-x, 2-y, -1-z$; (vi) $1+x, 1+y, -1+z$; (vii) $2-x, 2-y, -1-z$).

4. Database survey

A search of the Cambridge Crystallographic Database (CSD, Version 5.41 updated to March 2020; Groom *et al.*, 2016) using the fragments 2-, 3- and 4-carboxypyridine-*N*-oxide yielded 20 hits, of which 16 were complexes of 4-carboxypyridine-*N*-oxide, three contained 3-carboxypyridine-*N*-oxide, including the prior report of the title compound, and one contained 2-carboxypyridine-*N*-oxide. The last (IJOHAR; Wang *et al.*, 2011) is also a polymeric Cu^{II} complex in which the organic ligand chelates through one carboxylate oxygen and the *N*-oxide oxygen and bridges to two adjacent metals through the other carboxylate oxygen and the *N*-oxide oxygen. The other two complexes of 3-carboxypyridine-*N*-oxide are $[Dy(H_2O)$(3-carboxypyridine-*N*-oxide)(squarate)$]_n$ (OXOROK; Liu *et al.*, 2016) in which the 3-carboxypyridine-*N*-oxide chelates to one metal through the carboxyl group and bridges to a second through the *N*-oxide oxygen and $[Tb_2$(3-carboxypyridine-*N*-oxide)$_4(H_2O)_2$(oxalate)$]_n$ (QUBKEF; Yu *et al.*, 2015). The complexes of 4-carboxypyridine-*N*-oxide include a dinuclear Cu^{II} complex containing bidentate bridging and monodentate carboxylate ligands in which the *N*-oxide oxygen is not coordinated (BULWIO; Knuutilla, 1983) and a polymeric Cu^{II} complex in which all three oxygen atoms of the carboxylate ligand are involved in bridging coordination modes (YISLAQ; Ghosh *et al.*, 2018).

5. Hirshfeld surface analysis

An effective means of probing intermolecular interactions is Hirshfeld surface analysis (McKinnon *et al.*, 2007; Spackman & Jayatilaka, 2009), which can be conveniently carried out

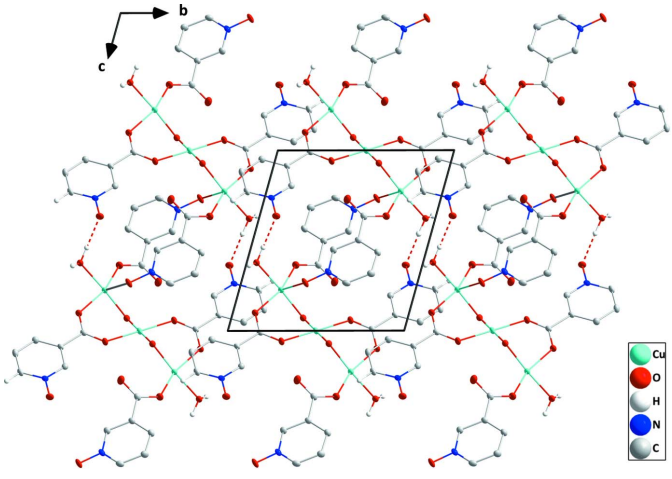

Figure 2
Plan view of one layer seen along the *a*-axis direction with O—H···O hydrogen bonds depicted by dashed lines.

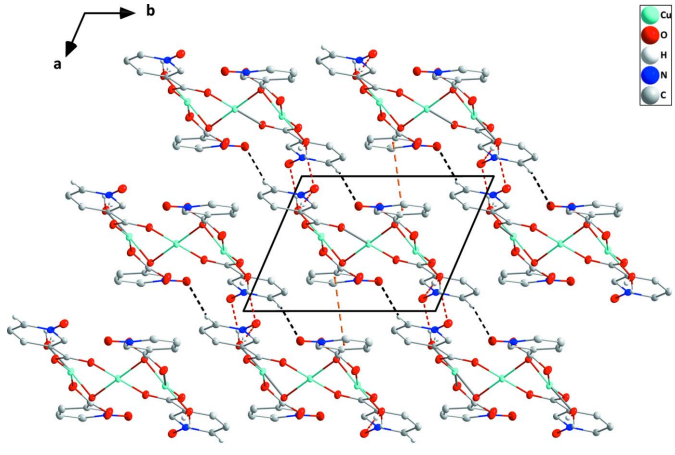

Figure 3
Elevation view of a portion of two layers seen along the *c*-axis direction and showing the π-stacking interactions (orange dashed lines) holding them together. O—H···O and C—H···O hydrogen bonds within layers are depicted by red and black dashed lines, respectively.

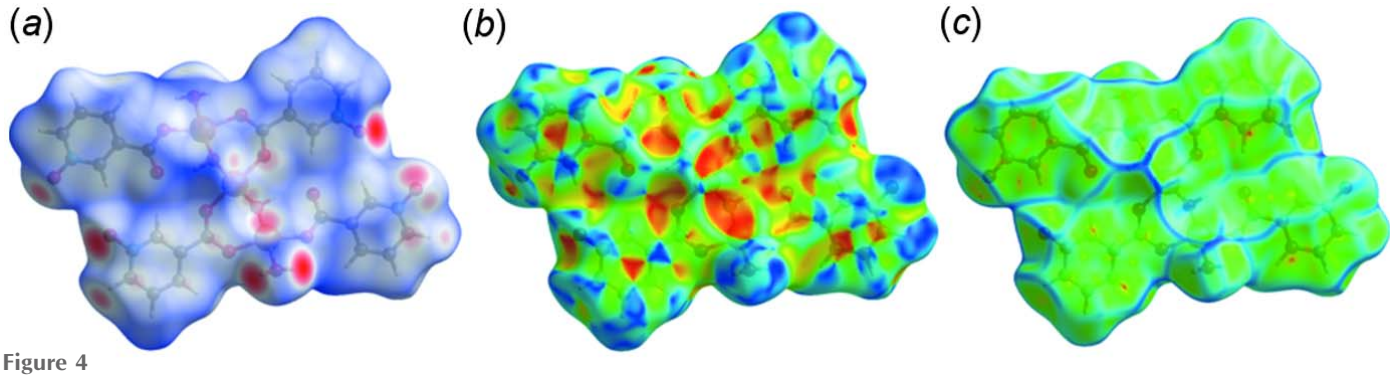

Figure 4
The Hirshfeld surface plotted over (*a*) d_{norm}, (*b*) shape index and (*c*) curvature.

with *Crystal Explorer 17* (Turner *et al.*, 2017). A detailed description of the use of *Crystal Explorer 17* and the plots obtained has been published (Tan *et al.*, 2019) so will not be given here. Fig. 4*a* presents the surface mapped over d_{norm} over the range −0.7162 to 1.5102 arbitrary units in which the bright-red spots indicate the strong O—H···O hydrogen bonds and the lighter red spots the weaker C—H···O hydrogen bonds listed in Table 2. Mapping of the Hirshfeld surface over shape-index is illustrated in Fig. 4*b* and provides a picture of possible π-stacking interactions. These are indicated by red–orange triangles surrounded by blue triangles, which occur over the pyridine rings, confirming the slipped π-stacking interaction discussed in Section 3. This is also indicated by the surface mapped over curvature (Fig. 4*c*) where the substantially flat regions of the plot again occur over the pyridine rings. Parsing the intermolecular interactions into specific types is accomplished with the fingerprint plots (Fig. 5). Fig. 5*a* shows the full fingerprint plot while Fig. 5*b* presents the H···O/O···H interactions which, not surprisingly, constitute the largest of the intermolecular interactions at 35.8% of the total. These are followed by H···H (Fig. 5*c*, 25.9%), H···C/C···H (Fig. 5*d*, 10.8%) and O···Cu (Fig. 5*e*, 10.8%) interactions. Not shown are the C···C (7.9%) and H···N/N···H (2.5%) contacts, with the former corresponding primarily to the slipped π-stacking interactions.

6. Synthesis and crystallization

An aqueous solution of $CuCl_2{\cdot}2H_2O$ (0.034 g, 0.2 mmol in 3.5 mL) was added to an aqueous solution (3.5 mL) containing pyridine-2,3-dicarboxylic acid (0.04 g, 0.2 mmol) and NaOH (0.2 ml, 1 mol L^{-1}), the mixture was stirred at 333 K for 2 h and then cooled to room temperature. After standing for a week, the light-blue precipitate that formed was filtered off and dried. Dark-blue, block-like crystals were obtained by slow evaporation of a solution of the precipitate in 5 mL of distilled water at room temperature. (yield: 30.61% based on Cu). Analysis calculated for: C, 27.00; H, 1.94; N, 4.50%. Found: C, 26.86; H, 2.02; N, 4.46%. IR (cm^{-1} KBr): 445, 489, 547, 612, 674, 688, 768, 798, 948, 1019, 1044, 1130, 1225, 1376, 1408, 1441, 1564, 1594, 1619, 2994, 3043, 3069, 3355.

7. Refinement

Crystal data, data collection and structure refinement details are summarized in Table 3. H atoms attached to carbon were placed in idealized locations (C—H = 0.95 Å) and were included as riding contributions with U_{iso}(H) = 1.2U_{eq}(C). Those attached to oxygen were placed in locations obtained from a difference map and were refined with DFIX O—H = 0.84 (1) Å restraints.

Funding information

JTM thanks Tulane University for support of the Tulane Crystallography Laboratory.

References

Balzarini, J., Stevens, M., De Clercq, E., Schols, D. & Pannecouque, C. (2005). *J. Antimicrob. Chemother.* **55**, 135–138.

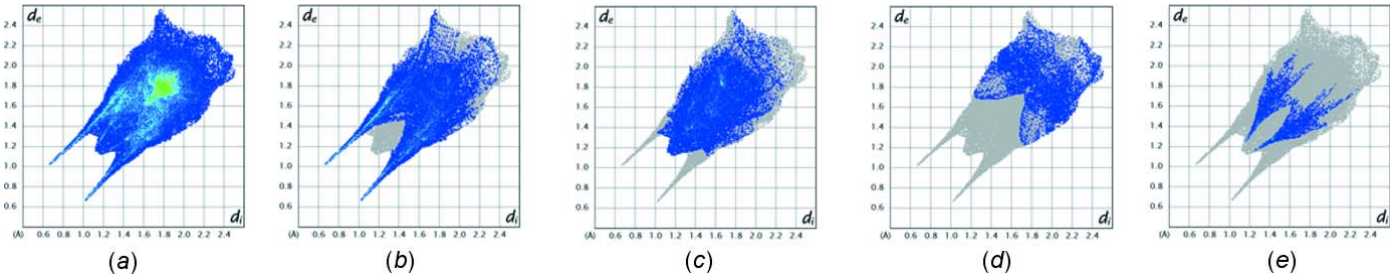

Figure 5
Fingerprint plots showing (*a*) all intermolecular interactions and resolved into (*b*) H···O/O···H, (*c*) H···H, (*d*) H···C/C···H and (*e*) O···Cu/Cu···O contacts.

Table 3
Experimental details.

Crystal data	
Chemical formula	$[Cu_3(C_6H_4NO_3)_4(OH)_2(H_2O)_2]$
M_r	813.07
Crystal system, space group	Triclinic, $P\overline{1}$
Temperature (K)	150
a, b, c (Å)	7.8669 (17), 9.710 (2), 10.424 (2)
α, β, γ (°)	97.016 (3), 110.701 (3), 109.049 (3)
V (Å^3)	678.2 (2)
Z	1
Radiation type	Mo $K\alpha$
μ (mm^{-1})	2.42
Crystal size (mm)	0.31 × 0.25 × 0.22
Data collection	
Diffractometer	Bruker *SMART APEX* CCD
Absorption correction	Multi-scan (*SADABS*; Krause *et al.*, 2015)
T_{min}, T_{max}	0.50, 0.62
No. of measured, independent and observed [$I > 2\sigma(I)$] reflections	12893, 3592, 3390
R_{int}	0.021
(sin $\theta/\lambda)_{max}$ (Å^{-1})	0.685
Refinement	
$R[F^2 > 2\sigma(F^2)]$, $wR(F^2)$, S	0.023, 0.065, 1.06
No. of reflections	3592
No. of parameters	226
No. of restraints	3
H-atom treatment	H atoms treated by a mixture of independent and constrained refinement
$\Delta\rho_{max}$, $\Delta\rho_{min}$ (e Å^{-3})	0.52, −0.31

Computer programs: *APEX3* and *SAINT* (Bruker, 2016), *SHELXT* (Sheldrick, 2015*a*), *SHELXL2018/1* (Sheldrick, 2015*b*), *DIAMOND* (Brandenburg & Putz, 2012) and *SHELXTL* (Sheldrick, 2008).

Bazargan, M., Mirzaei, M., Aghamohamadi, M., Tahmasebi, M. & Frontera, A. (2020). *J. Mol. Struct.* **1202**, 127243.
Bazargan, M., Mirzaei, M., Eshtiagh-Hosseini, H., Mague, J. T., Bauzá, A. & Frontera, A. (2016). *Inorg. Chim. Acta*, **449**, 44–51.
Bernstein, J., Davis, R. E., Shimoni, L. & Chang, N.-L. (1995). *Angew. Chem. Int. Ed. Engl.* **34**, 1555–1573.
Brandenburg, K. & Putz, H. (2012). *DIAMOND*, Crystal Impact GbR, Bonn, Germany.
Bruker (2016). *APEX3* and *SAINT*. Bruker AXS Inc., Madison, Wisconsin, USA.
Ghosh, D., Ferfolja, K., Drabavičius, Z., Steed, J. W. & Damodaran, K. K. (2018). *New J. Chem.* **42**, 19963–19970.
Groom, C. R., Bruno, I. J., Lightfoot, M. P. & Ward, S. C. (2016). *Acta Cryst.* B**72**, 171–179.
Hosseini Hashemi, Z., Mirzaei, M., Eshtiagh-Hosseini, H., Fereshteh, S., Shamsipur, M., Ardalani, M. & Blake, A. J. (2018). *J. Coord. Chem.* **71**, 4058–4071.
Hosseini-Hashemi, Z., Mirzaei, M., Jafari, A., Hosseinpour, P., Yousefi, M., Frontera, A., Lari Dashtbayaz, M., Shamsipur, M. & Ardalani, M. (2019). *RSC Adv.* **9**, 25382–25404.
Kang, Y.-F., Wang, Y.-L., Xu, L., Zhang, W.-Q., Cuo, L.-L. & Ma, Y.-M. (2020). *J. Solid State Chem.* **291**, 121260.
Knuutilla, H. (1981). *Inorg. Chim. Acta*, **50**, 221–225.
Knuutilla, H. (1983). *Inorg. Chim. Acta*, **72**, 11–16.
Krause, L., Herbst-Irmer, R., Sheldrick, G. M. & Stalke, D. (2015). *J. Appl. Cryst.* **48**, 3–10.
Laborda, S., Clérac, R., Anson, C. E. & Powell, A. K. (2004). *Inorg. Chem.* **43**, 5931–5943.
Lazarou, K. N., Savvidou, A., Raptopoulou, C. P. & Psycharis, V. (2018). *Polyhedron*, **152**, 125–137.
Lis, S., Hnatejko, Z., Barczynski, P. & Elbanowski, M. (2002). *J. Alloys Compd.* **344**, 70–74.
Liu, C.-M., Zhang, D., Hao, X. & Zhu, D.-B. (2016). *ACS Omega*, **1**, 286–292.
McKinnon, J. J., Jayatilaka, D. & Spackman, M. A. (2007). *Chem. Commun.* 3814–3816.
Mirzaei, M., Eshtiagh-Hosseini, H., Alipour, M., Bauzá, A., Mague, J. T., Korabik, M. & Frontera, A. (2015). *Dalton Trans.* **44**, 8824–8832.
Mirzaei, M., Eshtiagh-Hosseini, H. & Bazargan, M. (2015). *Res. Chem. Intermed.* **41**, 9785–9803.
Mirzaei, M., Eshtiagh-Hosseini, H., Bazargan, M., Mehrzad, F., Shahbazi, M., Mague, J. T., Bauzá, A. & Frontera, A. (2015). *Inorg. Chim. Acta*, **438**, 135–145.
Mirzaei, M., Sadeghi, F., Molčanov, K., Zaręba, J. K., Gomila, R. M. & Frontera, A. (2020). *Cryst. Growth Des.* **20**, 1738–1751.
Noro, S., Mizutani, J., Hijikata, Y., Matsuda, R., Sato, H., Kitagawa, S., Sugimoto, K., Inubushi, Y., Kubo, K. & Nakamura, T. (2015). *Nat. Commun.* **6**, 5851.
Procházková, S., Kubíček, V., Böhmová, Z., Holá, K., Kotek, J. & Hermann, P. (2017). *Dalton Trans.* **46**, 10484–10497.
Shahbazi, M., Mehrzad, F., Mirzaei, M., Eshtiagh-Hosseini, H., Mague, J. T., Ardalani, M. & Shamsipur, M. (2017). *Inorg. Chim. Acta*, **458**, 84–96.
Sheldrick, G. M. (2008). *Acta Cryst.* A**64**, 112–122.
Sheldrick, G. M. (2015*a*). *Acta Cryst.* A**71**, 3–8.
Sheldrick, G. M. (2015*b*). *Acta Cryst.* C**71**, 3–8.
Spackman, M. A. & Jayatilaka, D. (2009). *CrystEngComm*, **11**, 19–32.
Tan, S. L., Jotani, M. M. & Tiekink, E. R. T. (2019). *Acta Cryst.* E**75**, 308–318.
Turner, M. J., McKinnon, J. J., Wolff, S. K., Grimwood, D. J., Spackman, P. R., Jayatilaka, D. & Spackman, M. A. (2017). *Cryst. Explorer 17*. The University of Western Australia.
Wang, X.-Y., Zhang, X.-Q. & Wu, W.-S. (2011). *Acta Cryst.* E**67**, m225.
Xiong, Y., Fan, Y.-Z., Yang, R., Chen, S., Pan, M., Jiang, J.-J. & Su, C.-Y. (2014). *Chem. Commun.* **50**, 14631–14634.
Yu, Y., Zhang, L., Zhou, Y. & Zuhra, Z. (2015). *Dalton Trans.* **44**, 4601–4612.

supporting information

Acta Cryst. (2021). E**77**, 309-313 [https://doi.org/10.1107/S2056989021002000]

A redetermination of the structure and Hirshfeld surface analysis of poly[di-aquadi-μ-hydroxido-tetrakis(μ-nicotinato *N*-oxide)tricopper(II)]

Masoud Mirzaei, Maryam Bazargan, Pouria Ebtehaj and Joel T. Mague

Computing details

Data collection: *APEX3* (Bruker, 2016); cell refinement: *SAINT* (Bruker, 2016); data reduction: *SAINT* (Bruker, 2016); program(s) used to solve structure: *SHELXT* (Sheldrick, 2015*a*); program(s) used to refine structure: *SHELXL2018/1* (Sheldrick, 2015*b*); molecular graphics: *DIAMOND* (Brandenburg & Putz, 2012); software used to prepare material for publication: *SHELXTL* (Sheldrick, 2008).

Poly[diaquadi-μ-hydroxido-tetrakis(μ-pyridine-3-carboxylato *N*-oxide)tricopper(II)]

Crystal data

$[Cu_3(C_6H_4NO_3)_4(OH)_2(H_2O)_2]$
M_r = 813.07
Triclinic, $P\overline{1}$
a = 7.8669 (17) Å
b = 9.710 (2) Å
c = 10.424 (2) Å
α = 97.016 (3)°
β = 110.701 (3)°
γ = 109.049 (3)°
V = 678.2 (2) Å^3
Z = 1
$F(000)$ = 409
D_x = 1.991 Mg m^{-3}
Mo $K\alpha$ radiation, λ = 0.71073 Å
Cell parameters from 9998 reflections
θ = 2.3–29.1°
μ = 2.42 mm^{-1}
T = 150 K
Block, blue
0.31 × 0.25 × 0.22 mm

Data collection

Bruker SMART APEX CCD diffractometer
Radiation source: fine-focus sealed tube
Graphite monochromator
Detector resolution: 8.3333 pixels mm^{-1}
φ and ω scans
Absorption correction: multi-scan (*SADABS*; Krause *et al.*, 2015)
T_{min} = 0.50, T_{max} = 0.62
12893 measured reflections
3592 independent reflections
3390 reflections with $I > 2\sigma(I)$
R_{int} = 0.021
θ_{max} = 29.2°, θ_{min} = 2.2°
h = −10→10
k = −13→13
l = −14→14

Refinement

Refinement on F^2
Least-squares matrix: full
$R[F^2 > 2\sigma(F^2)]$ = 0.023
$wR(F^2)$ = 0.065
S = 1.06
3592 reflections
226 parameters
3 restraints
Primary atom site location: dual
Secondary atom site location: difference Fourier map
Hydrogen site location: mixed
H atoms treated by a mixture of independent and constrained refinement
$w = 1/[\sigma^2(F_o^2) + (0.0347P)^2 + 0.5335P]$ where $P = (F_o^2 + 2F_c^2)/3$

$(\Delta/\sigma)_{max}$ = 0.001
$\Delta\rho_{max}$ = 0.52 e Å^{-3}
$\Delta\rho_{min}$ = −0.31 e Å^{-3}

Special details

Experimental. The diffraction data were obtained from 3 sets of 400 frames, each of width 0.5° in ω, colllected at φ = 0.00, 90.00 and 180.00° and 2 sets of 800 frames, each of width 0.45° in φ, collected at ω = –30.00 and 210.00°. The scan time was 5 sec/frame.

Geometry. All esds (except the esd in the dihedral angle between two l.s. planes) are estimated using the full covariance matrix. The cell esds are taken into account individually in the estimation of esds in distances, angles and torsion angles; correlations between esds in cell parameters are only used when they are defined by crystal symmetry. An approximate (isotropic) treatment of cell esds is used for estimating esds involving l.s. planes.

Refinement. Refinement of F^2 against ALL reflections. The weighted R-factor wR and goodness of fit S are based on F^2, conventional R-factors R are based on F, with F set to zero for negative F^2. The threshold expression of $F^2 > 2\text{sigma}(F^2)$ is used only for calculating R-factors(gt) etc. and is not relevant to the choice of reflections for refinement. R-factors based on F^2 are statistically about twice as large as those based on F, and R- factors based on ALL data will be even larger. H-atoms attached to carbon were placed in calculated positions (C—H = 0.95 Å) while those attached to oxygen were placed in locations derived from a difference map and their coordinates adjusted to give O—H = 0.84 %A. The former were included as riding contributions with isotropic displacement parameters 1.2 times those of the attached atoms while the latter were refined subject to the restraint DFIX 0.84 (1).

Fractional atomic coordinates and isotropic or equivalent isotropic displacement parameters (Å^2)

	x	*y*	*z*	U_{iso}*/U_{eq}
Cu1	0.55161 (3)	0.76197 (2)	0.22674 (2)	0.01203 (6)
Cu2	0.500000	0.500000	0.000000	0.01188 (7)
O1	0.44050 (18)	0.71790 (14)	0.36494 (13)	0.0175 (2)
O2	0.2406 (2)	0.47108 (14)	0.27160 (14)	0.0245 (3)
O3	0.22121 (19)	0.36322 (14)	0.73304 (14)	0.0189 (2)
O4	0.38030 (18)	0.32089 (13)	0.05837 (12)	0.0146 (2)
O5	0.35598 (18)	0.12662 (13)	−0.09985 (12)	0.0154 (2)
O6	0.09294 (18)	0.09404 (14)	0.36357 (12)	0.0166 (2)
O7	0.35789 (17)	0.59314 (13)	0.07123 (12)	0.0126 (2)
H7A	0.308 (3)	0.534 (2)	0.110 (2)	0.029 (6)*
O8	0.74783 (18)	0.94425 (13)	0.37813 (12)	0.0152 (2)
H8A	0.788 (4)	0.931 (3)	0.4591 (16)	0.041 (8)*
H8B	0.848 (3)	0.981 (3)	0.362 (3)	0.035 (7)*
N1	0.2291 (2)	0.47710 (16)	0.67356 (14)	0.0135 (3)
N2	0.13829 (19)	0.03830 (15)	0.26216 (14)	0.0119 (2)
C1	0.3226 (2)	0.59140 (18)	0.36527 (17)	0.0138 (3)
C2	0.2845 (2)	0.59731 (18)	0.49796 (16)	0.0122 (3)
C3	0.2577 (2)	0.47220 (18)	0.55191 (17)	0.0136 (3)
H3	0.259212	0.383122	0.504107	0.016*
C4	0.2081 (2)	0.59753 (19)	0.73601 (17)	0.0155 (3)
H4	0.178573	0.595901	0.816802	0.019*
C5	0.2293 (3)	0.7225 (2)	0.68303 (17)	0.0171 (3)
H5	0.212768	0.806108	0.726578	0.020*
C6	0.2751 (2)	0.72616 (19)	0.56552 (17)	0.0152 (3)
H6	0.299241	0.814314	0.532209	0.018*
C7	0.3409 (2)	0.18427 (17)	0.00894 (16)	0.0111 (3)
C8	0.2615 (2)	0.07659 (17)	0.08634 (15)	0.0109 (3)

C9	0.2181 (2)	0.13269 (17)	0.19519 (16)	0.0117 (3)
H9	0.244784	0.237223	0.221998	0.014*
C10	0.0996 (2)	−0.11165 (18)	0.22703 (17)	0.0143 (3)
H10	0.043095	−0.176028	0.275773	0.017*
C11	0.1424 (2)	−0.17042 (18)	0.12053 (18)	0.0160 (3)
H11	0.115782	−0.275146	0.096237	0.019*
C12	0.2246 (2)	−0.07639 (18)	0.04886 (17)	0.0141 (3)
H12	0.254937	−0.115727	−0.024337	0.017*

Atomic displacement parameters (Å²)

	U^{11}	U^{22}	U^{33}	U^{12}	U^{13}	U^{23}
Cu1	0.01623 (11)	0.01106 (10)	0.01109 (10)	0.00360 (8)	0.00955 (8)	0.00412 (7)
Cu2	0.01632 (14)	0.01104 (13)	0.01417 (13)	0.00581 (10)	0.01150 (10)	0.00645 (10)
O1	0.0224 (6)	0.0161 (5)	0.0160 (5)	0.0030 (5)	0.0142 (5)	0.0056 (4)
O2	0.0389 (8)	0.0147 (6)	0.0243 (6)	0.0046 (5)	0.0241 (6)	0.0038 (5)
O3	0.0230 (6)	0.0195 (6)	0.0238 (6)	0.0098 (5)	0.0156 (5)	0.0165 (5)
O4	0.0201 (6)	0.0122 (5)	0.0169 (5)	0.0053 (4)	0.0138 (5)	0.0070 (4)
O5	0.0228 (6)	0.0136 (5)	0.0134 (5)	0.0048 (5)	0.0131 (5)	0.0053 (4)
O6	0.0206 (6)	0.0191 (6)	0.0132 (5)	0.0050 (5)	0.0132 (5)	0.0046 (4)
O7	0.0149 (5)	0.0125 (5)	0.0134 (5)	0.0043 (4)	0.0099 (4)	0.0044 (4)
O8	0.0211 (6)	0.0128 (5)	0.0131 (5)	0.0036 (5)	0.0113 (5)	0.0045 (4)
N1	0.0124 (6)	0.0157 (6)	0.0148 (6)	0.0050 (5)	0.0073 (5)	0.0090 (5)
N2	0.0125 (6)	0.0144 (6)	0.0099 (5)	0.0036 (5)	0.0069 (5)	0.0048 (5)
C1	0.0169 (7)	0.0156 (7)	0.0157 (7)	0.0087 (6)	0.0110 (6)	0.0075 (6)
C2	0.0118 (7)	0.0144 (7)	0.0123 (6)	0.0045 (6)	0.0070 (5)	0.0053 (5)
C3	0.0151 (7)	0.0144 (7)	0.0151 (7)	0.0060 (6)	0.0096 (6)	0.0059 (6)
C4	0.0158 (7)	0.0217 (8)	0.0118 (6)	0.0077 (6)	0.0078 (6)	0.0061 (6)
C5	0.0222 (8)	0.0187 (8)	0.0148 (7)	0.0106 (6)	0.0102 (6)	0.0047 (6)
C6	0.0190 (8)	0.0150 (7)	0.0153 (7)	0.0076 (6)	0.0096 (6)	0.0074 (6)
C7	0.0107 (7)	0.0135 (7)	0.0111 (6)	0.0041 (5)	0.0064 (5)	0.0060 (5)
C8	0.0110 (7)	0.0128 (7)	0.0105 (6)	0.0037 (5)	0.0063 (5)	0.0061 (5)
C9	0.0126 (7)	0.0116 (6)	0.0110 (6)	0.0025 (5)	0.0065 (5)	0.0046 (5)
C10	0.0142 (7)	0.0141 (7)	0.0172 (7)	0.0043 (6)	0.0087 (6)	0.0095 (6)
C11	0.0177 (8)	0.0128 (7)	0.0208 (8)	0.0064 (6)	0.0100 (6)	0.0078 (6)
C12	0.0161 (7)	0.0144 (7)	0.0153 (7)	0.0067 (6)	0.0094 (6)	0.0052 (6)

Geometric parameters (Å, º)

Cu1—O7	1.9003 (12)	N2—C9	1.3462 (19)
Cu1—O8	1.9539 (12)	N2—C10	1.360 (2)
Cu1—O1	1.9542 (12)	C1—C2	1.513 (2)
Cu1—O5^{i}	1.9911 (12)	C2—C3	1.386 (2)
Cu1—O3^{ii}	2.4208 (13)	C2—C6	1.396 (2)
Cu2—O7^{i}	1.9240 (11)	C3—H3	0.9500
Cu2—O7	1.9240 (11)	C4—C5	1.379 (2)
Cu2—O4	1.9687 (11)	C4—H4	0.9500
Cu2—O4^{i}	1.9688 (11)	C5—C6	1.395 (2)

O1—C1	1.276 (2)	C5—H5	0.9500
O2—C1	1.232 (2)	C6—H6	0.9500
O3—N1	1.3270 (17)	C7—C8	1.507 (2)
O4—C7	1.2541 (19)	C8—C12	1.393 (2)
O5—C7	1.2638 (19)	C8—C9	1.394 (2)
O6—N2	1.3381 (17)	C9—H9	0.9500
O7—H7A	0.819 (10)	C10—C11	1.381 (2)
O8—H8A	0.833 (10)	C10—H10	0.9500
O8—H8B	0.836 (10)	C11—C12	1.390 (2)
N1—C4	1.354 (2)	C11—H11	0.9500
N1—C3	1.362 (2)	C12—H12	0.9500

O7—Cu1—O8	176.16 (5)	O1—C1—C2	113.52 (14)
O7—Cu1—O1	97.79 (5)	C3—C2—C6	119.94 (14)
O8—Cu1—O1	84.60 (5)	C3—C2—C1	119.12 (14)
O7—Cu1—O5^{i}	92.38 (5)	C6—C2—C1	120.94 (14)
O8—Cu1—O5^{i}	84.42 (5)	N1—C3—C2	119.92 (15)
O1—Cu1—O5^{i}	158.98 (5)	N1—C3—H3	120.0
O7—Cu1—O3^{ii}	89.57 (5)	C2—C3—H3	120.0
O8—Cu1—O3^{ii}	92.82 (5)	N1—C4—C5	120.41 (15)
O1—Cu1—O3^{ii}	103.19 (5)	N1—C4—H4	119.8
O5^{i}—Cu1—O3^{ii}	95.20 (5)	C5—C4—H4	119.8
O7^{i}—Cu2—O7	180.0	C4—C5—C6	119.99 (15)
O7^{i}—Cu2—O4	92.31 (5)	C4—C5—H5	120.0
O7—Cu2—O4	87.69 (5)	C6—C5—H5	120.0
O7^{i}—Cu2—O4^{i}	87.69 (5)	C5—C6—C2	118.49 (15)
O7—Cu2—O4^{i}	92.31 (5)	C5—C6—H6	120.8
O4—Cu2—O4^{i}	180.00 (8)	C2—C6—H6	120.8
C1—O1—Cu1	128.46 (11)	O4—C7—O5	127.42 (14)
N1—O3—Cu1^{ii}	125.82 (9)	O4—C7—C8	116.01 (13)
C7—O4—Cu2	129.98 (10)	O5—C7—C8	116.56 (14)
C7—O5—Cu1^{i}	125.97 (10)	C12—C8—C9	119.83 (14)
Cu1—O7—Cu2	106.58 (6)	C12—C8—C7	121.94 (14)
Cu1—O7—H7A	102.7 (18)	C9—C8—C7	118.19 (14)
Cu2—O7—H7A	104.7 (18)	N2—C9—C8	119.81 (14)
Cu1—O8—H8A	115 (2)	N2—C9—H9	120.1
Cu1—O8—H8B	110.4 (19)	C8—C9—H9	120.1
H8A—O8—H8B	106 (3)	N2—C10—C11	120.03 (14)
O3—N1—C4	118.78 (13)	N2—C10—H10	120.0
O3—N1—C3	120.31 (14)	C11—C10—H10	120.0
C4—N1—C3	120.91 (14)	C10—C11—C12	120.01 (15)
O6—N2—C9	118.69 (13)	C10—C11—H11	120.0
O6—N2—C10	119.75 (13)	C12—C11—H11	120.0
C9—N2—C10	121.54 (14)	C11—C12—C8	118.77 (15)
O2—C1—O1	127.26 (15)	C11—C12—H12	120.6
O2—C1—C2	119.22 (14)	C8—C12—H12	120.6

Cu1^{ii}—O3—N1—C4	−133.95 (13)	Cu2—O4—C7—O5	−5.8 (3)

Cu1^{ii}—O3—N1—C3	46.08 (19)	Cu2—O4—C7—C8	175.93 (10)
Cu1—O1—C1—O2	−6.2 (3)	Cu1^{i}—O5—C7—O4	0.0 (2)
Cu1—O1—C1—C2	174.06 (10)	Cu1^{i}—O5—C7—C8	178.24 (10)
O2—C1—C2—C3	35.0 (2)	O4—C7—C8—C12	−175.48 (15)
O1—C1—C2—C3	−145.22 (15)	O5—C7—C8—C12	6.0 (2)
O2—C1—C2—C6	−144.61 (17)	O4—C7—C8—C9	6.8 (2)
O1—C1—C2—C6	35.1 (2)	O5—C7—C8—C9	−171.71 (14)
O3—N1—C3—C2	−173.87 (14)	O6—N2—C9—C8	−178.18 (13)
C4—N1—C3—C2	6.2 (2)	C10—N2—C9—C8	0.5 (2)
C6—C2—C3—N1	−2.3 (2)	C12—C8—C9—N2	−0.9 (2)
C1—C2—C3—N1	178.07 (14)	C7—C8—C9—N2	176.91 (13)
O3—N1—C4—C5	175.41 (15)	O6—N2—C10—C11	178.72 (14)
C3—N1—C4—C5	−4.6 (2)	C9—N2—C10—C11	0.1 (2)
N1—C4—C5—C6	−0.8 (3)	N2—C10—C11—C12	−0.2 (2)
C4—C5—C6—C2	4.5 (3)	C10—C11—C12—C8	−0.2 (2)
C3—C2—C6—C5	−2.9 (2)	C9—C8—C12—C11	0.8 (2)
C1—C2—C6—C5	176.69 (15)	C7—C8—C12—C11	−176.96 (14)

Symmetry codes: (i) −*x*+1, −*y*+1, −*z*; (ii) −*x*+1, −*y*+1, −*z*+1.

Hydrogen-bond geometry (Å, º)

D—H···*A*	*D*—H	H···*A*	*D*···*A*	*D*—H···*A*
O7—H7*A*···O2	0.82 (1)	2.04 (1)	2.8057 (17)	156 (2)
O8—H8*A*···O6^{ii}	0.83 (1)	1.84 (1)	2.6684 (17)	173 (3)
O8—H8*B*···O6^{iii}	0.84 (1)	1.88 (1)	2.6976 (18)	168 (3)
C9—H9···O2	0.95	2.28	3.216 (2)	168
C10—H10···O3^{iv}	0.95	2.23	3.079 (2)	148

Symmetry codes: (ii) −*x*+1, −*y*+1, −*z*+1; (iii) *x*+1, *y*+1, *z*; (iv) −*x*, −*y*, −*z*+1.